IEEE Access
Multidisciplinary ⋮ Rapid Review ⋮ Open Access Journal

Received January 15, 2020, accepted February 23, 2020, date of publication March 2, 2020, date of current version March 11, 2020.

Digital Object Identifier 10.1109/ACCESS.2020.2977323

Positive Sequence Current Phase-Based Improved Reverse-Power Protection and a PV Hosting Capacity Assessment Method for Spot Networks

ZHIHUA ZHANG[1], (Member, IEEE), KUN WANG[1], QIANPENG ZHAO[2], YONGTAO TIAN[3], AND LIANGHUAN LI[4]

[1]College of New Energy, China University of Petroleum, Qingdao 266580, China
[2]Yuhang District Power Supply Company of State Grid Corporation of China, Hangzhou 311100, China
[3]College of Science, China University of Petroleum, Qingdao 266580, China
[4]Linyi Power Supply Company of State Grid Corporation of China, Linyi 276000, China

Corresponding author: Zhihua Zhang (zzh-upc@163.com)

This work was supported in part by the National Natural Science Foundation of China under Grant 51977220, in part by the Natural Science Foundation of Shandong Province under Grant ZR2019MEE057, and in part by the Fundamental Research Funds for the Central Universities under Grant 18CX05025A.

ABSTRACT A spot network is a special low-voltage distribution network with multiple sources supplying it in parallel. It can significantly enhance supply reliability and is beneficial for integrating a distributed energy resource (DER). However, because traditional reverse power protection in spot networks cannot identify the reverse power cause, DERs, especially photovoltaic (PV) hosting capacity, are limited. Meanwhile, no uniform method exists for assessing the PV injection capacity in spot networks. Based on comparing the positive sequence current phase, this article presents an improved reverse power protection and PV hosting capacity assessment method for spot networks. Current variation is adopted to identify the reverse power cause, and a spot network equivalent model with PV is built. The positive sequence current phase relationship at the reverse power protection location is analysed when different types of short circuit faults occur. A short circuit fault section can be determined by comparing the positive sequence current phase. The influence of the PV output current on the improved reverse power protection performance is analysed. Then, a PV hosting capacity assessment method with improved reverse power is presented based on the PV influence on protection instead of on node voltage. A simulation model based on an actual project is constructed using PSCAD software. The simulation results show that the improved reverse power protection significantly enhances the ability to inject PV into the spot network and operates correctly under faults. The theoretical PV hosting capacity agrees with the simulation results.

INDEX TERMS Spot network, reverse power protection, photovoltaic, hosting capacity, assessment method.

I. INTRODUCTION

The rapid development of the social economy, has caused the need reliable electrical supply to become increasingly urgent [1], [2]. Medium voltage (MV) distribution networks are usually operated in a radial configuration Equipped with simple and inexpensive protection and control measurements [3]. However, the load will suffer short interruptions when the fault section is isolated and while the normal area is recovered. Thus, it cannot meet the load demands and maintain a reliable supply [4], [5]. Meanwhile, distributed energy resource (DER), research—especially photovoltaic (PV), has been widely applied in recent years because of the energy crisis and environmental problems. However, PV usually operates with random and intermittent output characteristics; consequently, conventional distribution networks cannot incorporate PV in a friendly manner [6], [7]. This problem has become a major bottleneck that limits PV hosting capacity in distribution networks.

A spot network is a special low-voltage (LV) secondary network used in interconnected distribution networks. Generally, 3∼8 medium voltage feeders supply energy in parallel

The associate editor coordinating the review of this manuscript and approving it for publication was Guangya Yang.

to one spot network. Spot networks are considered the most reliable and flexible LV distribution mode for extremely important loads and they are beneficial for integrating PV [8]–[10]. Spot networks have been successfully used in the USA [11].

Generally, reverse power protection is set on the LV side to prevent loop power from occurring between the feeders. Reverse power protection can locate and isolate faults quickly when short-circuit faults occur in the feeders and can also improve the sensitivity of low-voltage side protection. However, the conventional reverse power protection and control method in spot networks cannot adopt friendly DER techniques, which seriously limits the PV hosting capacity.

Reverse power protection in the spot network is usually set to 0.1%–0.5% of the transformer capacity and does not consider the influence of injected PV [12], [13]. Thus, when PV is connected to a spot network, the traditional reverse power protection will misoperate frequently because of power fluctuations. Reverse power protection misoperation can be actively prevented by limiting the actual output power of PV [16]. An improved reverse power protection for spot networks with PV amounts was introduced in [13] based on the current variation and the power direction of the positive sequence fault component. This approach enhances operational reliability and is helpful for improving the PV hosting capacity. However, the PV hosting capability under this improved reverse power protection scheme was not analysed in detail. The authors of [14] constructed a reverse power protection method for a spot network that incorporated a reverse time-limit idea. This approach reduces the tripping probability caused by a power reversal. However, that study did not consider the inherent correlations between reverse power size and duration, load characteristics, PV output and other factors, or of protection settings. In [15], a reverse power protection method was proposed based on the idea of bus differential protection. This method improved the PV hosting capacity to a certain extent by utilizing all the power supply input, load and PV output information. However, there was no coordination between automatic reclosure and reverse power protection. The phenomenon of a ''switch jump'' still exists under large PV and load fluctuations. A power flow control method was presented in [16] to tackle the loop power problem. However, the influence of PV fluctuations on reverse power protection was not considered.

The ability to calculate the PV hosting capacity is critical to the design and operation of spot networks. The authors of [17] presented a method to determine the PV hosting capacity in a distribution network by considering a minimum load operation level constraint, and in [18], a maximum hosting capacity evaluation method was proposed. Several probabilistic indices were introduced in [19] to evaluate the potential operational effects of the increasing penetration of renewable DER units on rural distribution networks by evaluating technical benefits and risk tradeoffs. In [20], power quality variations and events that may arise due to high PV were assessed. This method considers the likely impacts due to DER integration under worst-case scenarios. In [21], a bilevel programming model was built to calculate the maximal allowable DER penetration capacity while considering load uncertainty and voltage constraints, and an active distribution network management approach was proposed in [22] to maximize DER hosting capacity. A novel method based on linear programming was proposed [23] to attenuate steady state over voltage problems and determine a good approximation of the maximum DER penetration level in radial distribution networks. The authors of [17]–[23] considered the maximal allowable DER penetration mainly from the perspective of the original system structure, which limits the development of DER access. However, the above research results did not address PV hosting capacity in spot networks with reverse power protection.

Based on comparing the positive sequence current phase, this article presents an improved method for reverse power protection and PV hosting capacity assessment in spot networks. Current variation is adopted to identify the reverse power cause. First, a spot network equivalent model is built that includes PV. Then, the positive sequence current phase relationship at the reverse power protection location is analysed when different types of short circuit faults occur. By comparing the positive sequence current phase, a short circuit fault section can be determined. The influence of the PV output current on the improved reverse power protection performance is analysed in detail. Then, a PV hosting capacity assessment method that includes the improved reverse power scheme is presented based on the influence of PV on protection instead of on node voltage. A simulation model based on an real project is constructed using PSCAD software. The simulation results show that the improved reverse power protection significantly enhances the ability to inject PV into a spot network that maintains correct operation under fault. The theoretical PV hosting capacity agrees with the simulation results.

II. COMPARING POSITIVE SEQUENCE CURRENT PHASE-BASED IMPROVED REVERSE POWER PROTECTION IN SPOT NETWORKS

A. TRADITIONAL REVERSE POWER PROTECTION IN SPOT NETWORKS

The feeders in a spot network, may have different equivalent source voltages and impedances. The load distribution on the medium voltage side may be uneven. This situation results in uneven output from each feeder and causes loop power to occur between each feeder. In severe cases, the power will be reversed in some feeders, greatly affecting the economy, stability and safety of system operation. Consequently, the low-voltage side of the spot network is generally configured with reverse power protection. In traditional reverse power protection, when reverse power is detected, the system judges that the feeder has a short circuit fault or loop power and sends a trip signal to the circuit breaker. This approach prevents loop power from occurring between feeders and improves the sensitivity of the low-voltage side protection.

However, traditional reverse power protection in spot networks is typically set to 0.1%–0.5% of the transformer capacity and does not consider the influence of injected PV. Therefore, when large amounts of PV are connected to the spot network, the traditional reverse power protection will misoperate frequently because of power fluctuations. Moreover, traditional reverse power protection systems are equipped with an automatic reclosing device, which may lead to the "jump" phenomenon, causing continuous tripping and closing of the circuit breaker and reducing the reliability of the spot network. Misoperation of reverse power protection can be actively prevented by limiting the actual output power of the PV; however, to some extent, that approach limits the development of PV in the spot network and is not conducive to fully utilizing renewable energy.

B. POSITIVE SEQUENCE CURRENT PHASE-BASED IMPROVED REVERSE POWER PROTECTION IN SPOT NETWORKS

The intermittent output of PV are mainly caused by the instability of primary energy; the fluctuating cycles of PV output power are determined by its energy varying characteristic. The durations of such variations are usually considerably longer than that of a fault—on the order of 1 s or more. However, the transient current under fault is very fast: on the order of 1 μs or even less. Obviously, there are clear differences between the current variations caused by PV fluctuation and those caused by system faults. Therefore, the cause of reverse power can be determined by assessing the current variation within a short time window.

Protection based on fault components has many advantages for analysing all types of faults, including overcoming the influence of load current, improving protection sensitivity, and so on. The limitation of PV injection in the distribution system is related to the minimum operational load [13]. In this article, the minimum load is assumed to be 0 kW. The PV hosting capacity is lower in this case. The positive sequence component is equal to the positive sequence fault component if a fault occurs at the moment a PV accesses the spot network. Therefore, in this study, a positive sequence component is used to design the reverse power protection theory instead of a fault component.

Because the number of feeders does not affect the fault characteristics of the spot network, three feeders are analysed as examples in this paper. An example spot network is shown in Fig. 1, where $\dot{U}_{Si}$ is the voltage of source I, Z_{Si} is the equivalent impedance of source I, Z_{li} is the equivalent impedance of Feeder i, i = 1-3, and f_1 and f_2 are the fault locations.

This spot network with a PV interface to the inverter can be simplified as shown in Fig. 2, where $\dot{U}_S$ is the source voltage, $Z_M = Z_S + Z_l$. Z_T is the equivalent impedance of each transformer, and Z_{LD} is the equivalent impedance of the load. The positive protection direction is defined from the feeder to the low-voltage bus, namely, $\dot{I}_{r-l1}$, $\dot{I}_{r-l2}$ and $\dot{I}_{r-l3}$, and $\dot{I}_{1-l1}$, $\dot{I}_{1-l2}$ and $\dot{I}_{r-l3}$ are the true current.

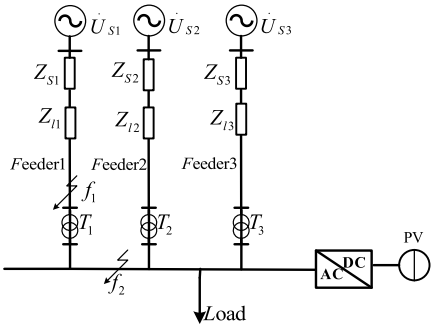

FIGURE 1. Spot network with PV and three feeders.

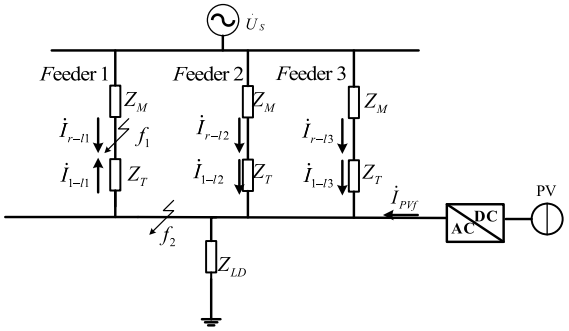

FIGURE 2. Equivalent circuit of a spot network with PV and three feeders.

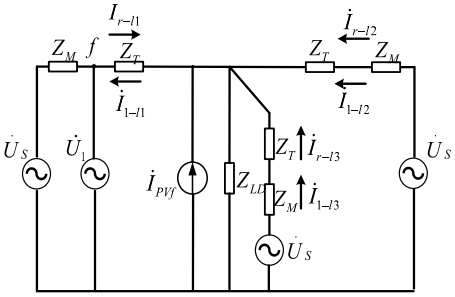

FIGURE 3. Positive sequence network under faults at Feeder 1 upstream.

When a fault occurs at f_1 in Fig. 2, namely, at MV Feeder 1, the current variations at various transformer secondary sides will exceed the protection threshold, and reverse power protection will launch. The positive sequence network diagrams under the three-phase short-circuit fault are shown in Fig. 3, and the positive sequence current phase relation of each feeder is shown in Fig. 4. With the reference phase of Feeder 1, the positive sequence current relationship between the normal feeders and the faulting Feeder 1 is as follows:

$$\begin{cases} 90° < arg\dfrac{\dot{I}_{1-l1}}{\dot{I}_{1-l2}} < 270° \\ 90° < arg\dfrac{\dot{I}_{1-l1}}{\dot{I}_{1-l3}} < 270° \\ -90° < arg\dfrac{\dot{I}_{1-l2}}{\dot{I}_{1-l3}} < 90° \end{cases}$$

The positive sequence current direction of the fault feeder is from the voltage bus to the fault point. The direction of the

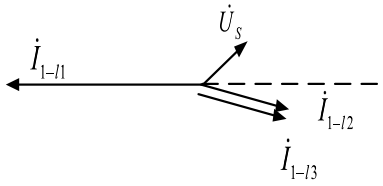

FIGURE 4. Phasor diagram of the positive sequence component under faults.

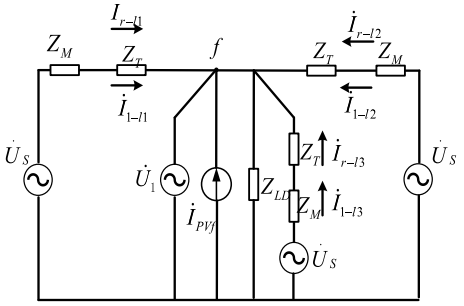

FIGURE 5. Positive sequence network under fault at the low-voltage bus downstream.

normal feeder is from the medium voltage feeder to the low voltage (LV) bus feeder. All the phase differences between the fault feeder and normal feeders meet these conditions, as shown in Equation (1). Then, the reverse power protection will trip the faulting feeder. Meanwhile, the phase difference of the positive sequence current between normal feeders does not satisfy Formula (1). The protection will not operate for the normal feeders; they will return automatically after a certain delay time:

$$90^\circ < arg\frac{\dot{I}_{li}}{\dot{I}_{lj}} < 270^\circ (1 \le i \le n;\ 1 \le j \le n \text{ and } j \ne i) \quad (1)$$

where $\dot{I}_{li}$ and $\dot{I}_{lj}$ are the current vectors of Feeders i and j as measured by the reverse power protection.

In addition, if the fault occurs at f_2 in Fig. 2, namely, at the LV bus bar, the positive sequence network diagrams under the three-phase short-circuit fault at the LV bus bar are shown in Fig. 5. The positive sequence current phase relation of each feeder is shown in Fig. 6. As can be seen from Figs. 5 and 6, the positive sequence current relationships between the feeders are as follows:

$$\begin{cases} -90^\circ < arg\dfrac{\dot{I}_{1-l1}}{\dot{I}_{1-l2}} < 90^\circ \\ -90^\circ < arg\dfrac{\dot{I}_{1-l1}}{\dot{I}_{1-l3}} < 90^\circ \\ -90^\circ < arg\dfrac{\dot{I}_{1-l2}}{\dot{I}_{1-l3}} < 90^\circ \end{cases}$$

The positive sequence current direction of all feeder protection points is from the LV bus to the fault point. None of these positive sequence current phases meets Equation (1); thus, the protection does not fire, and these feeders return automatically after a certain delay time.

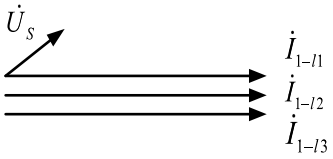

FIGURE 6. Phasor diagram of the positive sequence component under fault at the low-voltage bus.

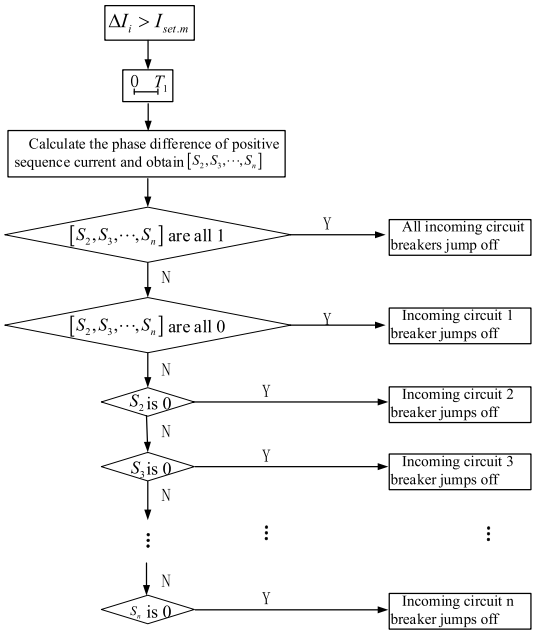

FIGURE 7. Logic diagram of improved reverse power protection based on comparing the positive sequence phase.

The fault location can be determined by comparing the phase differences of the positive sequence current between the two feeders. Under the condition of permissible PV permeability, equation (1) is the protection criterion to identify a short circuit fault feeder. To reduce the amount of required computation, the positive sequence current phase of a certain feeder can be taken as a reference value. Then, the phase differences between the other feeders and the reference feeder can be calculated. The operational logic of this reverse power protection in the spot network is shown in Fig. 7, where S_n is the phase difference between feeder N and the reference feeder. When the current phase difference between feeder N and the reference feeder is within the range of $-90^\circ \sim 90^\circ$, it is marked as a "1", and when it is within the range of $90^\circ \sim 270^\circ$, it is marked as a "0".

Compared with traditional reverse power protection, the improved reverse power protection judges the operational state via current variations. It takes the current variation as the starting amount of the protection, uses the positive sequence current phase to identify the fault location, and yields the setting principle and the protection realization logic. This protection method is effectively able identify the difference between reverse power caused by a feeder fault and larger variations in PV output, and it will not misoperate when the

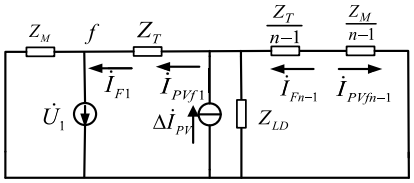

FIGURE 8. Positive sequence fault component equivalent network with a fault at f.

PV output is too large. Therefore, it can make full use of the advantages of spot networks in power supply reliability and PV-friendly access.

III. PV HOSTING CAPACITY ASSESSMENT METHOD IN SPOT NETWORKS WITH IMPROVED REVERSE POWER PROTECTION

Traditional reverse power protection relies solely on limiting the PV output to maintain reliable system operation. In this study, the influence of PV output on the positive sequence current phase is studied, and a method to assess PV hosting capacity assessment in spot networks that considers the improved reverse power protection method presented in this article is proposed.

A. INFLUENCE OF PV ACCESS TO REVERSE POWER PROTECTION PERFORMANCE

Generally, the output current of a PV inverter follows the positive sequence voltage phase at its access point. Its maximum output current amplitude is limited to $(1.2\sim1.5)I_N$, where I_N is the rated current of the PV inverter. The inverter control strategy usually affects the transient parameters. The reverse power protection in this paper uses the stable fault current, on which the PV control strategy has little influence.

According to [13], the equivalent network for the positive sequence fault component is as shown in Fig. 8 when the fault occurs at f. $\dot{U}_1$ is the positive sequence voltage fault component at fault location f, $\Delta\dot{I}_{PV}$ is the current variation of the PV inverter, $\dot{I}_{F1}$ is the positive sequence current fault component in the fault feeder, $\dot{I}_{Fn-1}$ is the corresponding fault current in the normal feeders. $\dot{I}_{PVf1}$ is the current variation caused by the PV inverter in the fault feeder, $\dot{I}_{PVfn-1}$ is the current variation in the normal feeders, and n is the number of feeders in the spot network. The other parameters are the same as those shown in Fig. 2.

As shown in Fig. 8, in the fault feeder, the direction of the current variation caused by the fault is the same as that caused by the PV. The direction of the positive sequence current fault component $\dot{I}_{Fn-1}$ caused by the fault is the opposite of the current direction $\dot{I}_{PVfn-1}$ by the PV output of the normal feeders. Therefore, the phase difference between the fault feeder and normal feeder increases with increasing PV output. When the PV output current is large enough, this phase difference will fail to meet Equation (1), and the corresponding reverse power protection will misoperate.

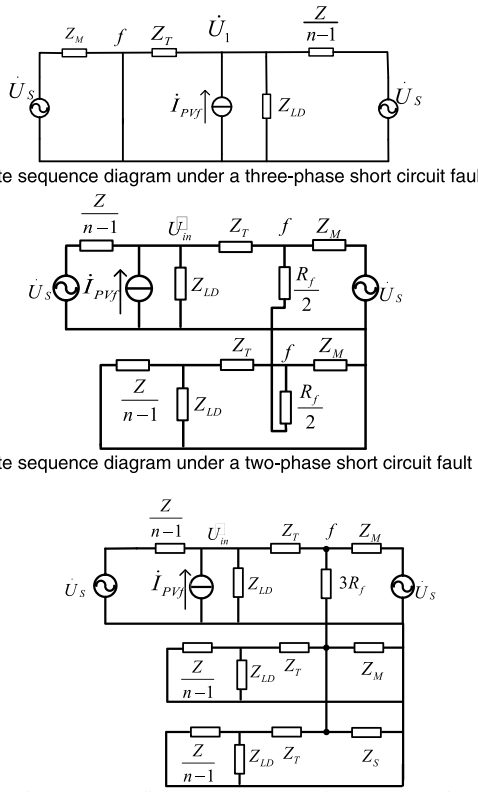

(a) Composite sequence diagram under a three-phase short circuit fault

(b) Composite sequence diagram under a two-phase short circuit fault

(c) Composite sequence diagram under a two-phase-to-ground short circuit fault

FIGURE 9. Composite sequence diagrams under different types of short circuit faults.

B. METHOD FOR ASSESSING PV TOLERANCE CAPACITY

Fig. 9 (a)–(c) shows the composite sequence network under different types of faults in the MV feeder, where $Z = Z_T + Z_S$. A single-phase ground fault on the MV side is not addressed in this paper; those types of fault characteristics are related to the neutral grounding mode.

Fig. 9 (a)–(c) can be simplified into a unified structure, as shown in Fig. 10. The equivalent compound sequence impedance Z_Δ includes positive, negative and zero sequence components, and is determined by the fault type as shown in Table 1

TABLE 1. Z_Δ expression under various types of fault.

Fault type	Z_Δ
Three phase short circuit fault	0
Two phase short circuit fault	$Z_f + R_f$
Two-phase-to-ground short circuit fault	$3R_f + \frac{Z_f}{2}$

where $Z_f = \frac{Z_M[ZZ_T+ZZ_{LD}+(n-1)Z_TZ_{LD}]}{Z(Z+nZ_{LD})}$.

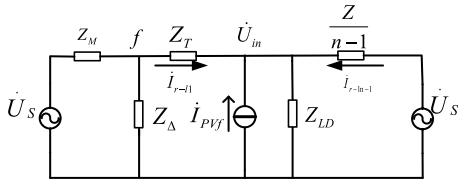

FIGURE 10. Unified compound sequence network under short circuit fault.

Suppose we have

$$\begin{cases} Z_1 = \dfrac{Z_\Delta Z_M}{Z_\Delta + Z_M} \\ Z_2 = \dfrac{Z_{LD}(Z_T + Z_1)}{Z_{LD} + Z_T + Z_1} \end{cases} \text{and} \quad \begin{cases} Z_3 = \dfrac{Z_{LD}Z/(n-1)}{Z_{LD} + Z/(n-1)} \\ Z_4 = \dfrac{Z_\Delta(Z_T + Z_3)}{Z_\Delta + Z_T + Z_3}. \end{cases}$$

According to the superposition theorem, the voltage $\dot{U}_{in}$ at the PV access point can be expressed as follows:

$$\dot{U}_{in} = \left(\frac{Z_2}{Z_2 + Z/(n-1)} + \frac{Z_4}{Z_4 + Z_S} \cdot \frac{Z_3}{Z_3 + Z_T}\right)\dot{U}_S + \frac{Z_2 Z/(n-1)}{Z_2 + Z/(n-1)}\dot{I}_{PVf} \quad (2)$$

Then, suppose that

$$\begin{cases} A_1 + jA_2 = \left(\dfrac{Z_2}{Z_2 + Z/(n-1)} + \dfrac{Z_4}{Z_4 + Z_M} \cdot \dfrac{Z_3}{Z_3 + Z_T}\right)\dot{U}_S \\ A_3 + jA_4 = \dfrac{Z_2 Z/(n-1)}{Z_2 + Z/(n-1)} \end{cases} \quad (3)$$

Generally, the output current of a PV inverter follows the phase of a positive sequence voltage at its injection point, namely,

$$\arg \dot{U}_{in} = \arg \dot{I}_{PVf}. \quad (4)$$

We set the phase of the positive sequence voltage at the injection point as θ. Then, substituting Equations (2) and (3) into Equation (4), we obtain Equation (5) as follows:

$$A_4 I_{PVf} = \sqrt{A_1^2 + A_2^2}\cos(\theta + \alpha). \quad (5)$$

where,

$$\begin{cases} \cos\alpha = -\dfrac{A_2}{\sqrt{A_1^2 + A_2^2}} \\ \sin\alpha = -\dfrac{A_1}{\sqrt{A_1^2 + A_2^2}} \end{cases}$$

The positive sequence current expressions of the fault feeder and normal feeders are

$$\begin{cases} \dot{I}_{1-l1} = -\dfrac{Z_\Delta \dot{U}_s}{(Z_4 + Z_M)(Z_\Delta + Z_3 + Z_T)} - \dfrac{Z_3}{Z_1 + Z_3 + Z_T}\dot{I}_{PVf} \\ + \dfrac{Z_{LD}\dot{U}_s}{(Z_2 + Z/(n-1))(Z_L + Z_T + Z_1)} \\ \dot{I}_{1-ln-1} = \dfrac{Z_\Delta Z_{LD}\dot{U}_s}{(Z_4 + Z_M)(Z_\Delta + Z_3 + Z_T)(Z_{LD} + Z_3)} \\ - \dfrac{\dot{U}_s}{Z_2 + Z/(n-1)} - \dfrac{Z_{LD}(Z_1 + Z_T)}{(Z_1 + Z_3 + Z_T)(Z_{LD} + Z/(n-1))}\dot{I}_{PVf}. \end{cases} \quad (6)$$

Now suppose that

$$\begin{cases} B_1 + jB_2 = \dfrac{Z_\Delta}{(Z_4 + Z_M)(Z_\Delta + Z_3 + Z_T)} \cdot \dfrac{Z_{LD}}{Z_{LD} + Z_3}\dot{U}_S \\ \quad - \dfrac{1}{Z_2 + Z/(n-1)}\dot{U}_S \\ B_3 + jB_4 = -\dfrac{Z_1 + Z_T}{Z_1 + Z_3 + Z_T} \cdot \dfrac{Z_{LD}}{Z_{LD} + Z/(n-1)} \\ C_1 + jC_2 = -\dfrac{Z_\Delta}{(Z_4 + Z_M)(Z_\Delta + Z_3 + Z_T)}\dot{U}_S \\ \quad + \dfrac{Z_{LD}}{(Z_2 + Z/(n-1))(Z_{LD} + Z_T + Z_1)}\dot{U}_S \\ C_3 + jC_4 = -\dfrac{Z_3}{Z_1 + Z_3 + Z_T} \end{cases}$$

According to the operational principle of the improved reverse power protection, Equation (7) can be met:

$$\tan\left(\arg \dot{I}_{1-ln-1}\right) \cdot \tan\left(\arg \dot{I}_{1-l1}\right) = -1. \quad (7)$$

Substituting Equation (6) into Equation (7), we obtain Equation (8), as shown at the bottom of the next page, where,

$$\begin{cases} \cos\gamma = \dfrac{B_2C_4 + B_4C_2 + B_1C_3 + B_3C_1}{\sqrt{(B_2C_3 + B_3C_2 - B_1C_4 - B_4C_1)^2 + (B_2C_4 + B_4C_2 + B_1C_3 + B_3C_1)^2}} \\ \sin\gamma = -\dfrac{B_2C_3 + B_3C_2 - B_1C_4 - B_4C_1}{\sqrt{(B_2C_3 + B_3C_2 - B_1C_4 - B_4C_1)^2 + (B_2C_4 + B_4C_2 + B_1C_3 + B_3C_1)^2}} \end{cases}$$

According to the output characteristics of PV, assume that

$$I_{PVf} = 1.5 I_{PV}. \quad (9)$$

Now suppose that

$$\begin{cases} A = \sqrt{(B_2C_3 + B_3C_2 - B_1C_4 - B_4C_1)^2 + (B_2C_4 + B_4C_2 + B_1C_3 + B_3C_1)^2} \\ \sigma = -\dfrac{B_1C_1 + B_2C_2 + 2.25B_3C_3I_{PV}^2 + 2.25B_4C_4I_{PV}^2}{1.5 I_{PV} A} \end{cases}$$

Combining Equations (5), (8) and (9), the PV access limitation I_{PV} can be obtained as shown in Equation (10).

$$\arccos\left(\frac{1.5 I_{PV} A_4}{\sqrt{A_1^2 + A_2^2}}\right) - \arccos\sigma = \alpha - \gamma, \quad (10)$$

To guarantee the reliability of the reverse power protection operation, the PV hosting capacity can be obtained as follows:

$$I_{PV\,\mathrm{set}} = \mathrm{K}_{rel2} I_{PV\,\min}, \quad (11)$$

where $I_{PV\,\min}$ is the minimum limit of the PV maximum capacity tolerance under all types of short circuit conditions, $I_{PV\,\mathrm{set}}$ is the actual PV hosting capacity, and K_{rel2} is the reliability coefficient.

This approach improves the stability of the spot network system and is conducive to the development of distributed energy generation.

TABLE 2. Simulation parameters.

Element	Parameters
Source	$\dot{E}_{S1}=\dot{E}_{S2}=\dot{E}_{S3}=13.2\angle 90°kV$ $f=60HZ$
Feeder	$Z_{S1}=Z_{S2}=Z_{S3}=(1.122+j1.496)\times 10^{-3}\Omega$ $Z_{l1}=Z_{l2}=Z_{l3}=(0.8485+j0.8478)\Omega$
Transformer	$Z_{T1}=Z_{T2}=Z_{T3}=(2.98+j13.82)\times 10^{3}\Omega$ $k_1=k_2=k_3=13.2/0.48$ $S_{T1}=S_{T2}=S_{T3}=0.75MVA$
Transition resistance	$R_f=2\Omega$

IV. SIMULATION AND ANALYSIS

The simulation, which is based on PSCAD software, models an actual project at Colorado Convention Center in Denver, Colorado. The simulation model includes three MV feeders as shown in Fig. 11. The simulation parameters are listed in Table 2.

A. OPERATING PERFORMANCE OF TRADITIONAL REVERSE POWER PROTECTION

The traditional reverse power protection in the spot network is set to 0.5% of the transformer capacity, namely, 0.01 kW. When t = 1 s, PV is put into operation, and its output is gradually increased. The relationship between the active power and PV output current detected during the reverse power protection of feeders is shown in Fig. 12, where P1, P2 and P3 represent the positive sequence power detected by the three feeder relays. *IPV_a_RMS* is the effective value of the current output by the PV inverter. From Fig. 12, it can be seen that when the PV output current reaches approximately 0.46 kA, the reverse power detected at the protection site is approximately 0.01 kW. In other words, it reaches the threshold value of the traditional reverse power protection, causing the protection to misoperate.

B. IMPROVED OPERATING PERFORMANCE OF REVERSE POWER PROTECTION

To avoid the influence of low-voltage load start-up on positive sequence variation, the protection threshold is set based on the value of the current flowing through the protection when the low-voltage bus is connected to the maximum three-phase load:

$$I_{set}=\frac{\sqrt{2}}{N-1}K_{rel1}K_{ss}I_{L.\max}=\frac{\sqrt{6}K_{rel1}K_{ss}P_{\max}}{3\,(N-1)\,U_N\cos\phi},\quad(12)$$

where K_{rel1} is the reliability coefficient, K_{ss} is the starting coefficient of the load. $I_{L.\max}$ is the maximum unit load current, $P_{\max}$ is the maximum unit load power, U_N is the rated voltage at the low voltage bus bar, and $\cos\phi$ is the load power factor.

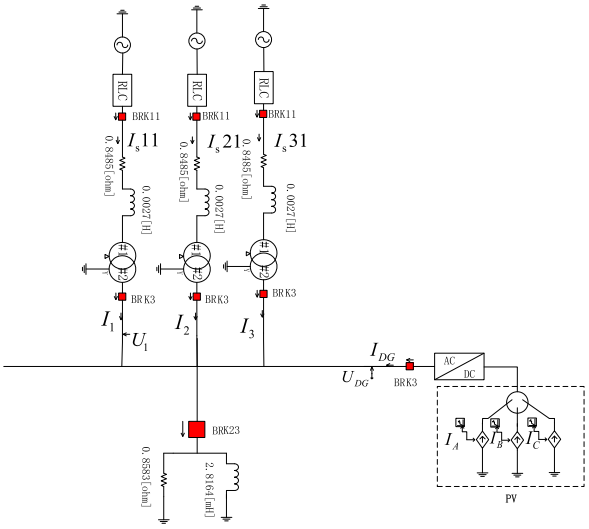

FIGURE 11. Simulation model structure.

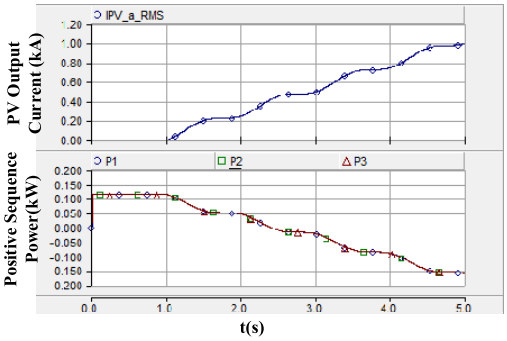

FIGURE 12. Output waveforms of the feeders and PVs.

Suppose that the maximum three-phase load of the low-voltage bus is 0.1 MW, the power factor is 0.85, the system has three feeders, and the equivalent voltage of the low-voltage side is 0.48 kVK_{rel1} = 1.1. The protection threshold can then be calculated according to Formula (12) as shown below:

$$I_{set}=\frac{\sqrt{6}\times 1.1\times 7\times 0.1}{3\times(3-1)\times 0.48\times 0.85}=0.77kA\quad(13)$$

When t = 1 s, the PV is accessed by the low voltage bus of the spot network, and its output is increased gradually. The PV output and the current variation are observed. The waveform is shown in Fig. 13, where △I1_1, △I2_1 and △I3_1 are the single-phase current variations of each feeder.

The traditional reverse power protection method misoperates when the output current of PV reaches 0.46 kA. From Fig. 13, the current variation is much less than the start-up setting value of the improved reverse power protection. Nevertheless, the protection does not start and will not misoperate.

$$\sqrt{(B_2C_3+B_3C_2-B_1C_4-B_4C_1)^2+(B_2C_4+B_4C_2+B_1C_3+B_3C_1)^2}\cdot I_{PVf}\cos(\theta+\gamma)=-(B_1C_1+B_2C_2+B_3C_3I_{PVf}^2+B_4C_4I_{PVf}^2)\quad(8)$$

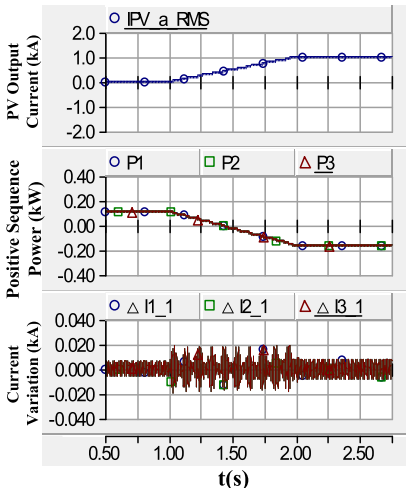

FIGURE 13. Waveforms of feeder output current variations and PV output.

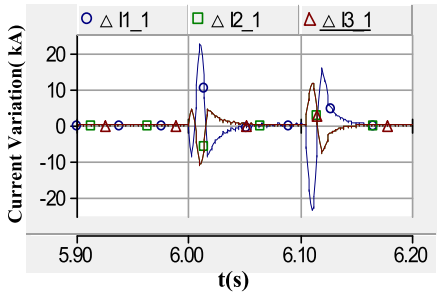

FIGURE 14. The instantaneous waveform of current variation under a three-phase fault occurring on Feeder 1.

Therefore, the reverse power protection method presented in this article allows a larger PV hosting capacity for a spot network system than does the traditional reverse power protection method. Namely, this improved reverse power protection can greatly enhance the PV hosting capacity.

A three-phase short circuit is taken as an example to verify that the improved reverse power protection operates reliably when a feeder fails. The short circuit fault occurs in Feeder 1 at 6 s. The circuit breaker operates at 6.1 s. The instantaneous waveform of current variation detected by the feeder relays at the secondary side is shown in Fig. 14. The phase difference of the positive sequence current between feeders is shown in Fig. 15, where ph12 is the phase difference of the positive sequence current between Feeder 1 and Feeder 2; ph13 is the phase difference between Feeder 1 and Feeder 3; and ph23 is the phase difference between Feeder 2 and Feeder 3.

As shown in Fig. 14, the current variation in each feeder exceeds the threshold value and the improved reverse power protection starts.

From Fig. 15, for a fault in Feeder 1, both ph12 and ph13 satisfy Equation (1); consequently, the improved reverse power protection trips the circuit breaker. However, for Feeders 2 and 3, ph23 does not satisfy Equation (1) and the protection does not operate. Therefore, it can reliably isolate fault points.

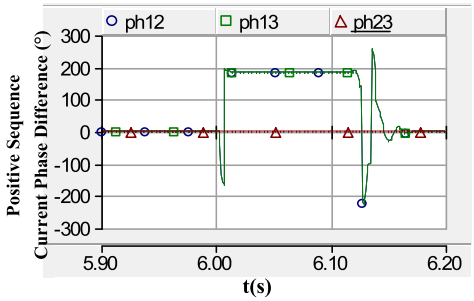

FIGURE 15. Positive sequence current phase difference under a three-phase fault.

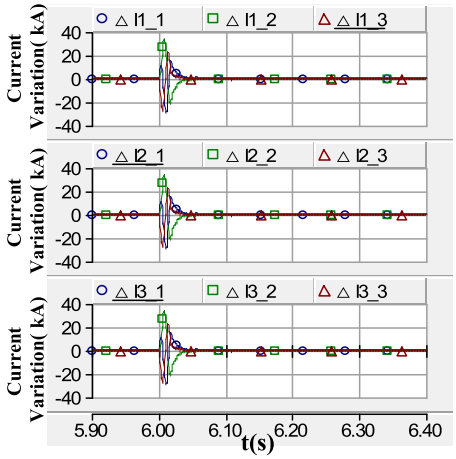

FIGURE 16. The instantaneous waveform of current variation under the three-phase short-circuit fault occurring at the LV bus bar.

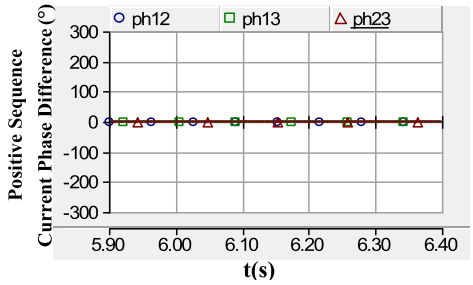

FIGURE 17. The instantaneous waveform of the positive sequence current phase difference under various faults at the LV bus bar.

In this case, the short circuit fault occurs in the low voltage bus at 6 s. The instantaneous waveform of the current variation detected by the incoming relays is shown in Fig. 16, and the phase difference of the positive sequence current between the feeders is shown in Fig. 17.

As shown in Fig. 16, the current variation in each feeder exceeds the threshold; therefore, the improved reverse power protection starts.

Finally, as shown in Fig. 17, none of ph12, ph13 and ph23 satisfy Equation (1). Consequently, the protection does not start, and the improved reverse power protection will not misoperate.

To verify the reliability of the improved reverse power protection, the maximum load and capacitor are used as interference. The capacitance compensation is set to 30% of

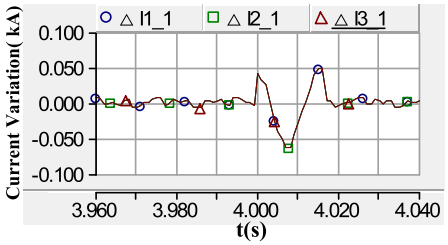

FIGURE 18. Current variation during the maximum motor starting.

TABLE 3. Theoretical value of PV tolerance capacity in each short-circuit fault state (Unit: KA).

Fault type	PV tolerance capacity
$f^{(3)}$	22.62
$f^{(2)}$	9.16
$f_R^{(2)}$	4.75
$f^{(1,1)}$	12.86
$f_R^{(1,1)}$	9.73

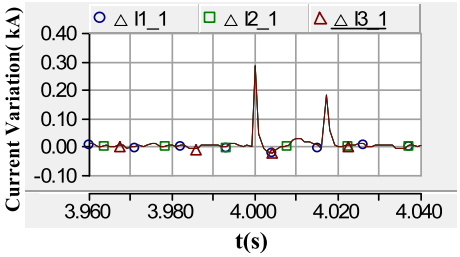

FIGURE 19. Current variation during the capacitor input.

the load capacity, namely, 0.105 kVar. When t = 4 s, the system experiences maximum load, and the current variation is shown in Fig. 18. When t = 4 s, the capacitor is put into the system, and the current variation is shown in Fig. 19.

As seen from Figs. 18 and 19, when the maximum load and capacitor are put into the system, the current variation remains well below the threshold for protection. In this case, the improved reverse power protection will not misoperate.

C. VERIFICATION OF THE ASSESSMENT METHOD FOR PV TOLERANCE CAPACITY

Based on Equations (4) and (8) and the simulation parameters in Table 2, the coefficient in Equation (12) can be obtained, and the PV access limitation can be calculated under different fault conditions by solving Equation (10), as shown in Table 3, where $f^{(3)}$ is a three-phase short circuit fault, $f^{(2)}$ is a two-phase short circuit fault, $f_R^{(2)}$ is a two-phase short circuit fault with a transient resistance of 2 Ω, $f^{(1,1)}$ is a two-phase to ground short circuit fault, and $f_R^{(1,1)}$ is a two-phase ground short circuit fault with a transient resistance of 2 Ω. A single-phase ground fault on the MV side is not addressed in this paper because its fault characteristics are related to the neutral grounding mode.

To prove that the PV capacity limitation is a boundary condition for reverse power protection operation, the relationship between the positive sequence current phase of feeders

TABLE 4. Phase information corresponding to the corresponding PV tolerance capacity (Unit: Degree).

Fault type	$\varphi_{\dot{I}_{1-l1}}$	$\varphi_{\dot{I}_{1-l2}}$	$\varphi_{\dot{I}_{1-l3}}$	$\varphi_{\frac{\dot{I}_{1-l2}}{\dot{I}_{1-l1}}}$	$\varphi_{\frac{\dot{I}_{1-l3}}{\dot{I}_{1-l1}}}$
$f^{(3)}$	-65.44	24.69	24.69	90.13	90.13
$f^{(2)}$	261.77	-8.21	-8.21	90.02	90.02
$f_R^{(2)}$	268.31	-1.83	-1.83	89.86	89.86
$f^{(1,1)}$	267.65	-3.14	-3.14	89.21	89.21
$f_R^{(1,1)}$	264.03	-5.58	-5.58	90.39	90.39

TABLE 5. Phase Information of the positive sequence current under various faults in feeder 1 (Unit: Degree).

Fault type	$\varphi_{\dot{I}_{1-l1}}$	$\varphi_{\dot{I}_{1-l2}}$	$\varphi_{\dot{I}_{1-l3}}$	$\varphi_{\frac{\dot{I}_{1-l2}}{\dot{I}_{1-l1}}}$	$\varphi_{\frac{\dot{I}_{1-l3}}{\dot{I}_{1-l1}}}$
$f^{(3)}$	232.38	27.12	27.12	154.74	154.74
$f^{(2)}$	240.01	12.39	12.39	132.38	132.38
$f_R^{(2)}$	264.95	11.11	11.11	106.16	106.16
$f^{(1,1)}$	236.91	19.51	19.51	142.60	142.60
$f_R^{(1,1)}$	241.89	16.43	16.43	134.54	134.54

is simulated and shown in Table 4, where I_{1-l1} is the positive sequence current in fault feeders, I_{1-l2} is the positive sequence current in normal feeder 2, I_{1-l3} is the positive sequence current in normal feeder 3, $\varphi_{\frac{I_{1-l12}}{I_{1-l1}}}$ is the phase difference between $\dot{I}_{1-l2}$ and $\dot{I}_{1-l1}$, and $\varphi_{\frac{I_{1-l13}}{I_{1-l1}}}$ is the phase difference between $\dot{I}_{1-l3}$ and $\dot{I}_{1-l1}$.

The simulation result in Table 4 shows that the improved reverse power protection in the normal feeders might misoperate because $\varphi_{\frac{I_{1-l2}}{I_{1-l1}}}$ and $\varphi_{\frac{I_{1-l3}}{I_{1-l1}}}$ is near 90°. To enhance the reliability of the improved reverse power protection, the PV hosting capacity should be calculated according to Equation (12), where the reliability coefficient K_{rel2} is 0.85:

$$I_{PV\,\mathrm{set}} = \mathrm{K}_{rel2} I_{PV\,\mathrm{min}} = 4.04kA. \tag{14}$$

Namely, the maximum PV hosting capacity is 4.04 kA.

Suppose that the maximum three-phase load unit is 0.1 MW and its power factor is 0.85, $K_{rel1} = 1.1$, $K_{SS} = 7$. According to Equation (13), the operational value of the reverse power protection is $I_{set} = 0.77kA$. When a fault occurs at the feeder, the positive sequence current phase of reverse power protection is as shown in Table 5. This result shows that the improved reverse power protection with PV access maximum capacity can operate correctly and reliably. When a fault occurs at the secondary bus bar, the positive sequence current phase measured by all the reverse power protection is as listed in Table 6, which shows that the improved reverse power protection with PV access maximum capacity will not misoperate.

From the above analysis, it can be concluded that compared with the traditional reverse power protection, the improved reverse power protection does not directly judge the operational status of feeders by the reverse power. Instead, it allows

TABLE 6. Phase information of various faults occurring at the LV bus bar (Unit: Degree).

Fault type	$\varphi_{\dot{I}_{1-l1}}$	$\varphi_{\dot{I}_{1-l2}}$	$\varphi_{\dot{I}_{1-l3}}$	$\varphi_{\frac{\dot{I}_{1-l2}}{\dot{I}_{1-l1}}}$	$\varphi_{\frac{\dot{I}_{1-l3}}{\dot{I}_{1-l1}}}$
$f^{(3)}$	75.45	75.45	75.45	0	0
$f^{(2)}$	75.94	75.94	75.94	0	0
$f_R^{(2)}$	95.48	95.48	95.48	0	0

the spot network system to have reverse power, which can significantly improve the PV hosting capacity. The PV hosting capacity can be assessed based on the reverse power protection operation criterion.

V. CONCLUSION

In this article, a spot network equivalent model with PV is established and the characteristics of short circuit faults of feeders and low voltage buses are analysed. Combined with the principle of current variation, an improved reverse network power protection method based on positive sequence current phase comparison is proposed. Then, a PV hosting capacity assessment method based on this protection method is proposed, and the following conclusions are drawn:

1) Considering the PV injection limitation of traditional protection, the improved reverse power protection locates the fault section correctly by performing phase comparisons of the positive sequence fault component. This scheme allows reverse power due to the high PV output in spot networks during normal operation, which greatly enhances the PV penetration capability.

2) The PV hosting capacity assessment method based on the improved reverse power protection considers the influence of PV output on the characteristics of various short-circuit faults in the spot network, and the maximum PV hosting capacity of the system is derived. This method improves the stability of the spot network system and is conducive to the development of distributed energy generation.

3) The PV hosting capacity is closely related to the minimum load. The heavier the minimum load is, the larger the PV hosting capacity is.

REFERENCES

[1] Y. Zhang, L. Wang, and W. Sun, "Trust system design optimization in smart grid network infrastructure," *IEEE Trans. Smart Grid*, vol. 4, no. 1, pp. 184–195, Mar. 2013.
[2] A. O. Ohara, C. S. Takiguchi, B. Iwamoto, C. C. Teixeira, E. C. Belvedere, D. Varolo, C. Martins, R. O. Brandao, B. Mello, and R. F. Costa, "Reliability improvement on underground distribution spot network system," in *Proc. IEEE PES*, Apr. 2010, pp. 1–8.
[3] S. Junlakarn and M. Ilic, "Distribution system reliability options and utility liability," *IEEE Trans. Smart Grid*, vol. 5, no. 5, pp. 2227–2234, Sep. 2014.
[4] R. Langella, T. Manco, and A. Testa, "Unifying supply reliability and voltage quality in the representation of an electrical system node," *IEEE Trans. Power Del.*, vol. 25, no. 2, pp. 1172–1181, Apr. 2010.
[5] K. Chen, W. Wu, B. Zhang, S. Djokic, and G. P. Harrison, "A method to evaluate total supply capability of distribution systems considering network reconfiguration and daily load curves," *IEEE Trans. Power Syst.*, vol. 31, no. 3, pp. 2096–2104, May 2016.
[6] A. K. Basu, S. Chowdhury, and S. P. Chowdhury, "Impact of strategic deployment of CHP-based DERs on microgrid reliability," *IEEE Trans. Power Del.*, vol. 25, no. 3, pp. 1697–1705, Jul. 2010.
[7] W. Cao, J. Wu, N. Jenkins, C. Wang, and T. Green, "Benefits analysis of soft open points for electrical distribution network operation," *Appl. Energy*, vol. 165, pp. 36–47, Mar. 2016.
[8] *IEEE Standard for Interconnecting Distributed Resources with Electric Power Systems*, Standard 1547-2014, May 2014.
[9] E. Alegria, T. Brown, E. Minear, and R. H. Lasseter, "CERTS microgrid demonstration with large-scale energy storage and renewable generation," *IEEE Trans. Smart Grid*, vol. 5, no. 2, pp. 937–943, Mar. 2014.
[10] K. Anderson and M. A. B. K. Coddington, "Interconnecting PV on New York city's secondary network: Distribution system," Office Sci. Tech. Inf., Oak Ridge, TN, USA, Tech. Rep. DOE/GO/17062-1, 2009.
[11] M. Coddington, B. Kroposki, T. Basso, K. Lynn, and M. Vaziri, "Photovoltaic systems interconnected onto secondary network distribution systems," in *Proc. 34th IEEE Photovoltaic Specialists Conf. (PVSC)*, Jun. 2009, pp. 405–408.
[12] Z. Zhang, P. Crossley, and L. Li, "A positive-sequence-fault-component-based improved reverse power protection for spot network with PV," *Electr. Power Syst. Res.*, vol. 149, pp. 102–110, Aug. 2017.
[13] Z. Zhang, P. Crossley, B. Xu, and M. Yin, "Sequence current component and its power direction-based improved protection for spot network with DERs," *IET Gener., Transmiss. Distrib.*, vol. 11, no. 7, pp. 1634–1644, May 2017.
[14] D. R. Sevcik, "CenterPoint Energy 12 kV network feeder 'back feed' protective relaying," in *Proc. 67th Annu. Conf.* College Station, TX, USA, Apr. 2014, pp. 186–192.
[15] P. Mohammadi and S. Mehraeen, "Challenges of PV integration in low-voltage secondary networks," *IEEE Trans. Power Del.*, vol. 32, no. 1, pp. 525–535, Feb. 2017.
[16] Z. Zhang, B. Xu, and Y. Zhao, "Power flow distribution and its control technology for spot network with multi low-voltage sources parallel supply," *Autom. Electr. Power Syst.*, vol. 38, no. 2, pp. 59–63, 2014.
[17] *Stochastic Analysis to Determine Feeder Hosting Capacity for Distributed Solar PV*, EPRI, Palo Alto, CA, USA, 2011.
[18] M. S. S. Abad, J. Ma, D. Zhang, A. S. Ahmadyar, and H. Marzooghi, "Probabilistic assessment of hosting capacity in radial distribution systems," *IEEE Trans. Sustain. Energy*, vol. 9, no. 4, pp. 1935–1947, Oct. 2018.
[19] M. A. Akbari, J. Aghaei, M. Barani, M. Savaghebi, M. Shafie-Khah, J. M. Guerrero, and J. P. S. Catalao, "New metrics for evaluating technical benefits and risks of DGs increasing penetration," *IEEE Trans. Smart Grid*, vol. 8, no. 6, pp. 2890–2902, Nov. 2017.
[20] S. Pukhrem, M. Basu, and M. F. Conlon, "Probabilistic risk assessment of power quality variations and events under temporal and spatial characteristic of increased PV integration in low-voltage distribution networks," *IEEE Trans. Power Syst.*, vol. 33, no. 3, pp. 3246–3254, May 2018.
[21] K. Liu, Y. Liu, and W. Sheng, "Maximal allowable DG penetration capacity calculation considering voltage constraints," *Electr. Power Autom. Equip.*, vol. 36, no. 6, pp. 81–87, Jun. 2016.
[22] F. Ding and B. Mather, "On distributed PV hosting capacity estimation, sensitivity study and improvement," in *Proc. IEEE Power Energy Soc. Gen. Meeting (PESGM)*, Aug. 2018, pp. 1010–1020.
[23] M. S. S. Abad, G. Verbic, A. Chapman, and J. Ma, "A linear method for determining the hosting capacity of radial distribution systems," in *Proc. Australas. Universities Power Eng. Conf. (AUPEC)* Melbourne, VIC, Australia Nov. 2017, pp. 1–6.

ZHIHUA ZHANG (Member, IEEE) received the B.S. degree from Shijiazhuang Tiedao University, in 2001, the M.S. degree from the China University of Petroleum, Qingdao, China, in 2004, and the Ph.D. degree from Shandong University, China.

He is currently an Associate Professor with the College of New Energy, China University of Petroleum. He is the author of over 40 research articles in refereed journals and conference proceedings and has patented ten inventions. His research interests include flexible distribution technology and fault seamless self-healing technology.

KUN WANG is currently pursuing the bachelor's degree with the College of New Energy, China University of Petroleum, Qingdao, China.

His research interests include protection and fault analysis of AC/DC hybrid spot networks.

YONGTAO TIAN received the B.S. degree from Shijiazhuang Tiedao University, in 2001, and the M.S. degree from the Beijing University of Technology, Beijing, China, in 2004.

She is currently teaching with the College of Science, China University of Petroleum Qingdao, China. Her research interests include microelectronics and solid-state electronics.

QIANPENG ZHAO received the B.S. and M.S. degrees from the College of Information and Control Engineering, China University of Petroleum, Qingdao, China, in 2018.

She currently works for the Yuhang District Power Supply Company of the State Grid Corporation of China, Hangzhou. Her research interest includes reverse power protection for low voltage networks with multiple sources.

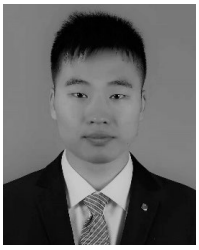

LIANGHUAN LI received the M.S. degree from the College of Information and Control Engineering, China University of Petroleum, Qingdao, China, in 2017.

He currently works for Linyi Power Supply Company of the State Grid Corporation of China, Linyi. His research interests include power system relay protection technology and distribution network automation technology.